

ARCHITECTURE CONSIDERATIONS FOR 60 GHz PULSE TRANSCEIVER FRONT-ENDS

M. Kraemer^{*,**}, A. Lecoindre^{*,**}, D. Dragomirescu^{*,**}, R. Plana^{*}

^{*}LAAS-CNRS, University of Toulouse, France

^{**}INSA Toulouse, Toulouse, France

E-mail: daniela@laas.fr

Abstract

While Impulse Ultra Wideband (I-UWB) is well established in the frequency range between 3.1 and 10.6 GHz, the application of pulse modulation in the frequency band around 60 GHz is a recent development. In this paper, the properties of 60 GHz pulses are outlined. Different architectures for pulse based transceiver front-ends are compared. It is distinguished between the up-conversion of UWB-pulses and their direct generation at millimeter-wave (mm-wave) frequencies. Both non-coherent and coherent receiver front-ends are considered. These considerations form the basis for a future 60 GHz UWB transceiver in 65 nm CMOS SOI that can be employed as part of a System on Chip (SoC) for sensor networks.

Keywords: UWB, millimeter-wave, 60 GHz, pulse, coherent

1. INTRODUCTION

The desired properties for wireless sensor networks are manifold [1]: Depending on the application, high data rate, multi-user capability, low probability of detection and/or interception and very low cost and power consumption are demanded. These requirements can be met by transceivers using pulse based modulation techniques [2]. Time Hopping (TH) Pulse Position Modulation (PPM) is hereby the most promising scheme [3].

Because of its inherently transient nature, pulse modulation needs large bandwidths. One possibility is therefore the use of the UWB frequencies between 3.1 and 10.6 GHz. However, this frequency range is already occupied by other narrowband signals like WLAN, resulting in both a high interference level and a low permitted transmit power. The recent bulletin of the regulatory bodies in Europe constrains the use of parts of this frequency range even more.

Therefore, more and more research interest is focused on the frequency range around 60 GHz. Here, an unoccupied bandwidth of at least 7 GHz is available in the US, Europe and Japan with very high emission limits not likely to be exceeded by fully integrated transceivers. [4], [5].

Other advantages of this frequency range are a potentially high user density due to strong signal attenuation, small device dimensions permitting a true SoC architecture, a strong line-of-sight path (possible with directive antennas having mm-dimensions) and small delay spread introduced by the channel. Alto-

gether, there is a potential for data-rates between 1 and 10 Gbit/s.

While the mm-wave range was until recently only accessible by expensive III-IV semiconductors, the suitability of SiGe [6], and later CMOS technologies [7],[8],[9] for fully integrated transceiver circuits was demonstrated. The presented transceiver front-ends are intended for up- and down-conversion of modulated baseband signals not further specified.

In the first explicit demonstration of pulse modulation at 60 GHz, baseband PPM pulse trains are simply up-converted. A transmitter of that kind was first implemented in a III-IV [10] and later in SiGe BiCMOS technology [11]. The employed receivers use non-coherent detection for the down-conversion of the UWB-pulses.

Very recently, pulse generators (PG) that emit true UWB-pulses directly at 60 GHz were demonstrated. The approach in [12] uses CMOS-technology to delay ultra-short pulses and arrange a 60 GHz pulse, while in [13] an injection-locked oscillator is rapidly switched on and off.

The paper at hand will compare the different possibilities of pulse modulation techniques at 60 GHz. A *conversion approach* and a *direct approach* are explicitly distinguished. The principle architectures of the appropriate mm-wave front-ends are outlined. While up to date, the published receiver architectures for pulse modulation use *non-coherent* down-conversion methods, this paper shows the advantages and challenges of a carrier phase or pulse timing recovery.

In chapter 2 the characteristics of pulses at 3.1-10.6 GHz and 60 GHz are compared. In chapter 3 transmitter architectures for both approaches are presented. In chapter 4 the receiver principles are outlined. Chapter 5 gives some simulation results that compare coherent, correlation and non-coherent mm-wave front-ends.

Based on the simulation results and discussions in this paper, an architecture can be selected to build a PPM-TH-receiver in 65 nm CMOS SOI with superior performance.

2. PULSE WAVEFORMS

A simple PPM signal consisting of pulses with the constant pulse shape $g(t)$ can be described mathematically as [3]

$$s(t) = \sum_{k=-\infty}^{\infty} g(t - kT_d - \delta d_k), \quad (1)$$

with a pulse rate of $1/T_d$, a time delay between two adjacent pulse positions of δ , and the symbol to be transmitted at a discrete time instant k to be d_k . For sake of simplicity, TH is not included in (1).

In the 3.1 to 10.6 GHz band, a monocycle is a typical, simple pulse waveform $g(t)$ approximately meeting the spectrum requirements. Its representation in the time and frequency domain is given in figure 1. Note that due to its large relative bandwidth $b_{rel} > 100\%$ its characteristics are ultra-wideband with no oscillations occurring.

The pulse waveforms required for the 7 GHz range available at 60 GHz must look differently: because the relative bandwidth available is only $b_{rel} = 11.7\%$, a classical UWB waveform is not suited. The required waveform has narrowband, non-oscillating behaviour. A modulated Gaussian pulse meets these requirements. An example for such a pulse is depicted in Figure 2.

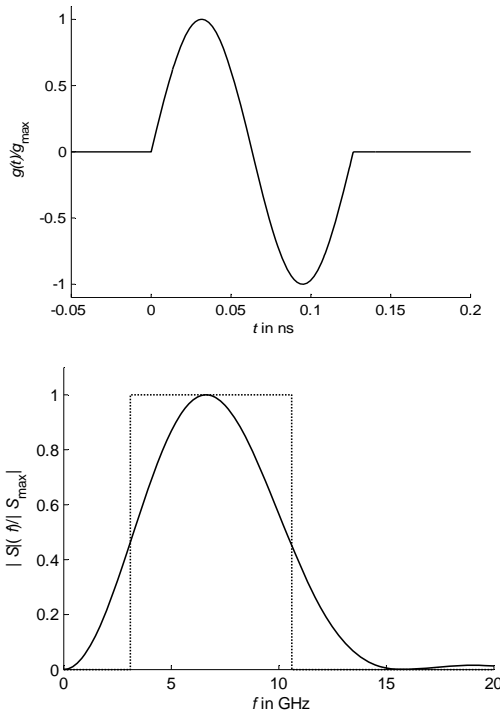


Figure 1: 3-10 GHz Monocycle and its normalized power density spectrum

Note the difference in mathematical representation between up-converted pulses and pulses directly generated at mm-waves: In the former case, the constant pulse waveform that is position-modulated is

$$g_1(t) = e^{-\left(\frac{t}{\tau}\right)^2}, \quad (2)$$

while in the latter the shifted pulse waveform is

$$g_2(t) = e^{-\left(\frac{t}{\tau}\right)^2} \cos(2\pi ft). \quad (3)$$

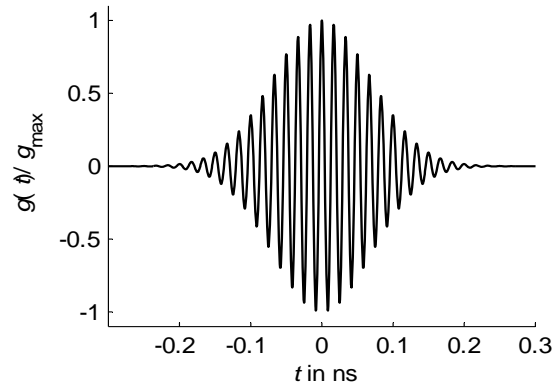


Figure 2: Gaussian-shaped 7 GHz-pulse $g(t)$ at 60 GHz

This implies that for PPM with true 60 GHz-pulses like $g_2(t)$ the sinusoid is shifted with the pulse position according to (1). This causes fundamental differences of the architectures of both transmitter and coherent receiver front-end between the conversion approach and the direct approach.

3. TRANSMITTER ARCHITECTURES

In this chapter, the two principle architectures for pulse transmitters are compared. It is always distinguished between the *conversion approach*, where baseband pulses like the one given in (2) are up-converted, and the *direct approach*, where pulses according to (3) are generated and transmitted directly at 60 GHz.

3.1. CONVERSION APPROACH

The block diagram of a transmitter using the conversion approach is sketched in Figure 3. The input signal of this transmitter is a PPM pulse train in the baseband with already shaped pulses $g_1(t)$. Alternatively, super-heterodyne-structures with one or more intermediate frequencies are possible, as well as lower oscillator frequencies that are multiplied to yield 60 GHz.

A modified version of this architecture is realized in [10] and [11]. There, the up-conversion is done by a switch instead of the mixer, necessitating a filter to shape the pulse at 60 GHz.

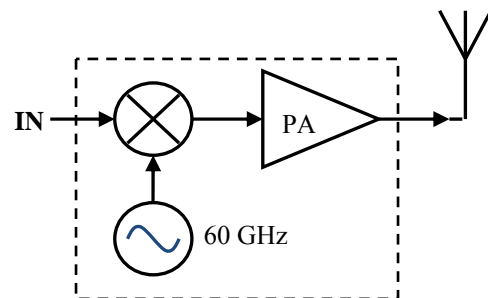


Figure 3: Millimeter-wave front-end for conversion approach

3.2 DIRECT APPROACH

At the direct approach the pulses are generated by a mm-wave pulse generator (PG), like the ones presented in [13], [14]. The input hereby is a digital pilot signal that designates the time instants when a pulse needs to be launched. The unifying property of all mm-wave PGs of this type is that the phase of the sinusoidal part of (3) always remains constant with respect to the maximum of the pulse. The transmitter principle for the direct approach is illustrated in figure 4.

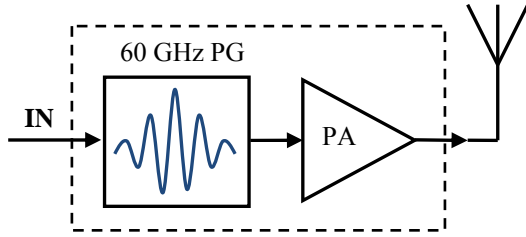


Figure 4: 60 GHz pulse transmitter

4. RECEIVER ARCHITECTURES

In this chapter receiver front-ends that facilitate the detection of the pulse positions in the baseband are shown. While the non-coherent down-conversion receiver works together with both transmitters, in chapter 4.2 and 4.3 receivers that are matched to the transmitter type are introduced.

4.1. NON-COHERENT APPROACH

In figure 5 the non-coherent receiver front-end is shown. The output-signal of this receiver yields the (noise-corrupted) envelope of the sent pulse train. If a additive white Gaussian noise (AWGN) channel with noise contribution $n(t)$ that corrupts the sent 60 GHz pulse $g_2(t)$ is assumed, the output signal (in front of the low-pass filter) is

$$\begin{aligned} & (g_2(t) + n(t))^2 \\ &= g_2(t)^2 + 2g_2(t)n(t) + n(t)^2. \end{aligned} \quad (4)$$

This signal contains a squared noise component. The same holds if the input signal originates from a conversion-approach transmitter, because no synchronization with the 60 GHz carrier phase is achieved.

The following two chapters propose architectures that synchronize either the carrier phase or the position of the 60 GHz pulses in order to reduce the noise contribution.

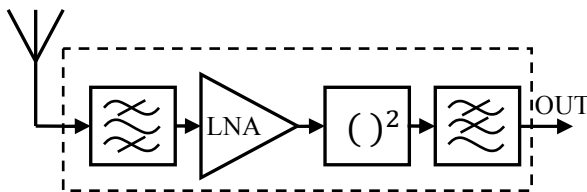


Figure 5 : Non-coherent detector front-end

4.2 CONVERSION APPROACH

The block diagram of a coherent receiver front-end for up-converted UWB-pulses is given in Figure 6. If carrier phase recovery can be accomplished, this circuit completely reconstructs the sent pulse train. Because the received signal, that is assumed to be only corrupted by the additive noise term $n(t)$, is multiplied with a uncorrupted, recovered carrier, the down-converted signal only contains a linear noise contribution:

$$(g_1(t) \cos(2\pi ft) + n(t))\cos(2\pi ft + \varphi) \quad (5)$$

The carrier phase recovery circuit that eliminates the phase difference φ can be accomplished by using feedback loops. A first PLL circuit at 60 GHz is demonstrated in [14] in BiCMOS SiGe technology.

Note that in contrast to the direct approach that will be presented in the following chapter, the down-converted baseband signal still needs to be analogly processed, i.e. by matched filtering.

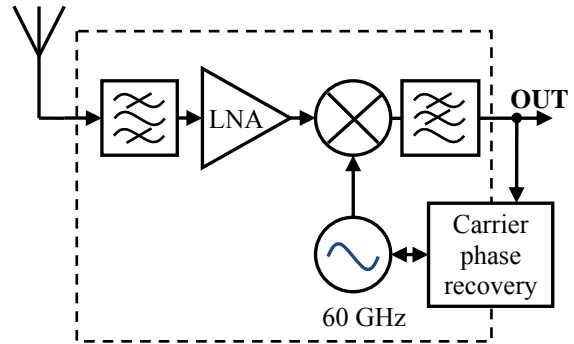


Figure 6: Coherent receiver front-end for up-converted UWB pulses

4.3 DIRECT APPROACH

The principal receiver structure for the direct approach is depicted in figure 7. The received 60 GHz pulses are not down-converted, but directly correlated with template pulses launched by a PG according to

$$\int_0^{T_0} (g_2(t) + n(t))g_2(t + t_0) dt \quad (7)$$

with T_0 being the duration of one pulse.

The challenge of this approach is to recover the pulse timing in order to determine when the template pulses need to be emitted: This will be accomplished for $t_0=0$ in (7). Different from the carrier phase recovery, where synchronization is done on one of the periodically occurring maxima of the auto-correlation function (ACF), the pulse timing recovery needs to detect the global maximum of the ACF. An example for an ACF of a 60 GHz pulse is depicted in figure 8 to illustrate the problem. A solution for this task was not

yet shown. Note that the output signal of this type of receiver is already matched-filtered and can be directly decided on.

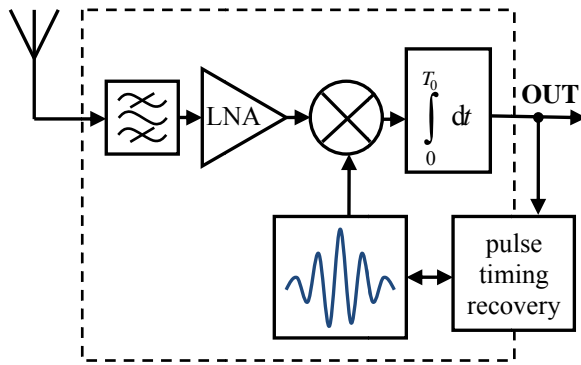


Figure 7: Correlation receiver for direct demodulation of 60 GHz pulses

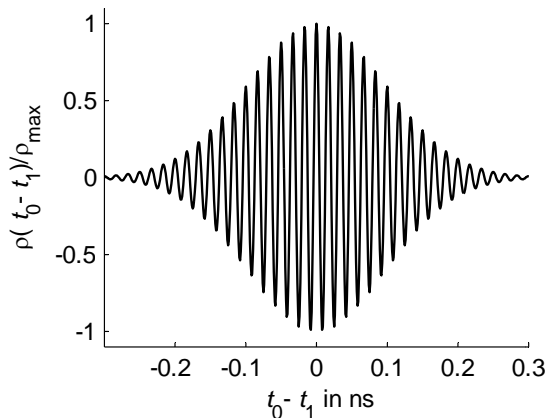


Figure 8 : Normalized ACF of a 60 GHz Gaussian pulse

5. SIMULATION RESULTS

In order to compare the performance of the presented receiver principles, the Bit Error Rate (BER) versus input Signal-to-Noise Ratio (SNR) was simulated in Matlab for a non-coherent receiver and the two ideally synchronized receivers. The results in Figure 9 show the benefits of synchronisation: The SNR is about 5 dB lower for the synchronized approaches when achieving the same BER.

6. CONCLUSIONS

Two different transceiver architectures, namely a direct approach and a conversion approach, were discussed. In addition to a non-coherent down-conversion of the received pulses, pulse receivers with synchronization were suggested. Simulations show a superior performance of these advanced architectures for pulse based modulations at 60 GHz.

For a future 65 nm CMOS SOI UWB transceiver one of the proposed architectures will be selected, depending on important properties of these circuits

like power consumption, size, realizability, back-end requirements and cost.

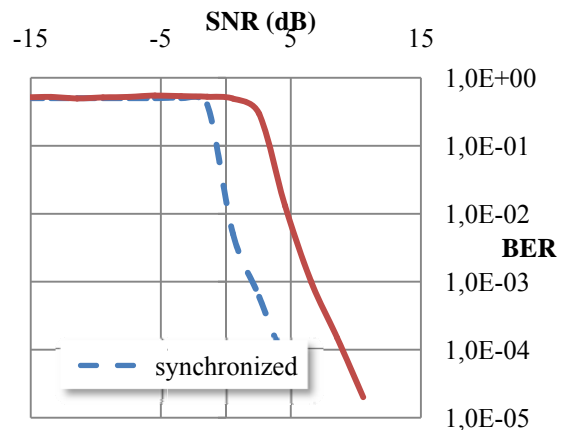


Figure 9: BER versus SNR for non-coherent detection and synchronous demodulation, 1Gbit/s

REFERENCES

- [1] Lecointre, A.; Dragomirescu, D. et al: "Miniaturized Wireless Sensor Networks", *International Semiconductor Conference, 2006*, p. 13-17
- [2] Win, M. & Scholtz, R.: "Impulse radio: how it works", *Communications Letters, IEEE*, 1998, p. 36-38
- [3] I. Oppermann, M. Hämäläinen, J. Iinatti: "UWB – Theory and Applications", John Wiley & Sons, Chichester, 2004
- [4] N. Guo, R.C. Qiu et al.: "60-GHz Millimeter-Wave Radio: Principle, Technology and New results", *EURASIP Journal on Wireless Communications and Networking*, 2007
- [5] Smulders, P.: "Exploiting the 60 GHz band for local wireless multimedia access: prospects and future directions", *IEEE Communications Magazine*, 2002, p.140-147
- [6] Reynolds, S.; Floyd, B.; Pfeiffer, U. & Zwick, T.: "60GHz transceiver circuits in SiGe bipolar technology", *ISSCC 2004, Digest of Technical Papers*. p. 442-538, Vol.1
- [7] Doan, C et al.: "Millimeter-wave CMOS design", *IEEE Journal of Solid-State Circuits*, 2005, p. 144-155
- [8] Razavi, B.: "A 60-GHz CMOS receiver front-end", *IEEE Journal of Solid-State Circuits*, 2007, p. 17-22
- [9] Alldred, D.; Cousins, B. & Voinigescu, S.: "A 1.2V, 60-GHz radio receiver with on-chip transformers and inductors in 90-nm CMOS", *IEEE Compound Semiconductor Integrated Circuit Symposium, 2006*, p. 51-54
- [10] Deparis, N et al.: "Transposition of a base band ultra wide band width impulse radio signal at 60 GHz for high data rates multiple access indoor communication systems", *34th European Microwave Conference, 2004*, p. 105-108
- [11] M. Devulder et al.: "Conception de circuits 60 GHz pur système Ultra Large Bande en technologie BiCMOS SiGe", *JNM 2007*
- [12] Badalawa, B. & Fujishima, M.: "60 GHz CMOS pulse generator", *IEEE Electronics Letters*, 2007, p.100-102
- [13] Deparis, N. et al.: "Module radio millimétrique utilisant la synchronisation d'une source 30 GHz par des trains d'impulsions ULB en bande de base", *JNM 2007*
- [14] Winkler, W.; Borngraber, J.; Heinemann, B. & Herzel, F.: "A fully integrated BiCMOS PLL for 60 GHz wireless applications", *ISSCC 2005*, p. 406-407, Vol.1